40. ROCK MAGNETISM OF IGNEOUS ROCKS FROM DEEP SEA DRILLING PROJECT SITES 482, 483, AND 485[1]

Ron Day and Mary Osterhoudt, University of California, Santa Barbara, California
and
Ulrich Bleil, Institut für Geophysik, Ruhr-Universität, Bochum, Postfach 10 21 48, West Germany

During DSDP Leg 65, we achieved significant basement penetration at three sites (482, 483, and 485) in the mouth of the Gulf of California (Lewis and Robinson, this volume). Since these holes were all drilled into extremely young crust near the crest of the East Pacific Rise, the rocks we recovered present an unusual opportunity to study the magnetic properties of submarine basalts before alteration has become pervasive. To take advantage of this opportunity and to complement the paleomagnetic studies conducted on these basalts by Day (this volume), we have studied, in the same samples, the following properties: saturation magnetization (J_s); intensity and stability of isothermal remanent magnetization (IRM); hysteresis parameters, such as the coercive force (H_C), the remanent coercive force (H_{RC}), and the ratio of saturation remanence (J_{RS}) to saturation magnetization; susceptibility (χ); and Curie temperature (T_c). In this chapter we will discuss the results of these studies in conjunction with the opaque mineralogy of the samples.

METHOD

With the exception of thermomagnetic analysis and microscope observations, we conducted studies of the samples' magnetic properties at the Rock Magnetism Laboratory, University of California, Santa Barbara.

We took the remanent magnetization measurements before and after AF demagnetization on a Schönstedt spinner magnetometer. Samples were progressively demagnetized to at least 10% of their initial intensity with a Schönstedt single-axis demagnetizer. We studied the acquisition of isothermal remanent magnetization in selected samples from each hole before these were given in a saturation isothermal remanent magnetization. Hysteresis loops were obtained using a vibrating sample magnetometer similar to that described by Kobayashi and Fuller (1967). From each loop we read saturation magnetization, coercive force, and the ratio of saturation remanence to saturation magnetization. The remanent coercive force was obtained from the direct field demagnetization of the saturation remanence. Susceptibility was measured both aboard ship (Day, this volume) and on an AC susceptibility bridge. All of the instruments can accommodate standard paleomagnetic cores (2.54 cm diameter × 2.54 cm length).

Thermomagnetic curves were measured at the Institut für Geophysik, Ruhr-Universität, Bochum, using an automatic recording magnetic-translation balance with an applied field of 2.5 kOe. All measurements were made in argon to a maximum temperature of about 625°C at heating and with a cooling rate of 40°C/min. The extremely low oxygen fugacity atmosphere effectively prevents oxidation of the magnetic oxides. As illustrated in Figure 1A, Curie temperatures were determined using a simple graphic technique (Grommé et al., 1963). As an aid to interpreting the thermomagnetic data, we examined polished sections of selected samples under reflected light using a Leitz Ortholux Pol microscope.

RESULTS

The magnetic properties we studied are listed in Table 1 in order of increasing depth in each hole for all of the samples studied. Also shown in Table 1 are the Curie temperatures of the samples in polished section and the values of natural remanent magnetization (J_{NRM}), stable inclination (I_0), and the Koenigsberger ratio (Q), presented by Day (this volume) for the same samples.

Thermomagnetic Analysis

We selected 37 samples for thermomagnetic analysis. The Curie temperatures found during heating and cooling are listed in Table 1, and Figure 1 shows typical thermomagnetic curves. As has been found in most other studies of oceanic basalts, the thermomagnetic curves reflect both reversible and irreversible behavior and a wide range of Curie temperatures. With few exceptions only one Curie temperature is observed per sample, indicating the presence of what is essentially a single phase magnetic mineral. None of the samples exhibited a truly reversible curve, but as in previous studies, a curve is considered reversible if the Curie temperature between the heating and cooling limbs differs by less than 50°C and if only minor changes (< 20%) in magnetization occur between the initial and final room-temperature magnetization. Figure 1A, for example, shows a reversible thermomagnetic curve.

Though most commonly associated with samples in which the Curie temperature is low (< 250°C), reversible curves are also associated with samples that have intermediate or high Curie temperatures (e.g., Sections 482C-11-1, 97 cm and 482D-8-1, 106 cm, respectively), and an approximately reversible curve was obtained for one of the samples (Section 482B-16-1, 117 cm) that displayed two Curie temperatures (Fig. 1C).

In contrast, about 30% of the thermomagnetic curves are clearly irreversible, and the Curie temperatures determined from the heating and cooling limbs differ by up to 277°C. Figures 1B and 1D are typical examples of this behavior. Without exception, samples whose curves were irreversible exhibited a lower Curie temperature and a decrease in magnetization upon cooling. This behavior is not typical of oceanic basalts; in most studies, the irreversible thermomagnetic curves are characterized by an initial Curie temperature between 200°C and

[1] Lewis, B. T. R., Robinson, P., et al., *Init. Repts. DSDP*, 65: Washington (U.S. Govt. Printing Office).

Table 1. Magnetic properties and Curie temperatures of basalts from Sites 482, 483, and 485.

Sample (level in cm)	Vol. (cm^3)	Depth (m)	J_{NRM} ($\times 10^{-3}$ gauss)	I (°)	MDF(1) (Oe)	J_{RS} (gauss)	MDF(2) (Oe)	J_S (gauss)	J_{RS}/J_S	H_C (Oe)	H_{RC} (Oe)	H_{RC}/H_C	χ ($\times 10^{-3}$ gauss)	Q	T_c (heating) (°C)	T_c (cooling) (°C)
Hole 482B																
11-1, 21	12.16	137.21	9.37	40		0.352	24	2.51	0.14	34	54	1.59	2.87	7.3		
11-2, 41	11.91	138.91	7.43	35	68	0.411	35	2.94	0.14	42	76	1.81	2.76	6.0	208	135
11-3, 15	11.91	140.15	9.75	40	35	0.259	20	1.99	0.13	25	41	1.64	3.18	6.8	108	92
12-1, 63	11.91	139.63	26.4	32	50	0.512	35	2.33	0.22	45	62	1.38	1.96	30.0		
12-2, 143	11.91	141.93	18.9	31	40	0.380	30	2.24	0.17	34	53	1.56	2.57	16.3	144	98
13-1, 126	11.91	145.26	10.1	33	62	0.417	35	2.98	0.14	42	67	1.60	2.33	9.7		
14-1, 97	11.40	148.97	17.2	25	317	0.573	270	1.17	0.49	225	312	1.39	0.55	69.6	234	127
14-3, 126	11.91	152.26	13.8	28	47	0.343	33	1.63	0.21	45	60	1.33	1.57	19.6		
15-1, 16	11.91	157.16	19.1	24	68	0.521	43	1.68	0.31	68	83	1.22	1.25	34.0		
15-2, 39	11.91	158.89	10.2	25	48	0.476	30	2.27	0.21				1.89	12.0		
15-3, 114	11.91	161.14	8.61	28	32	0.361	30	2.12	0.17	37	60	1.62	2.26	8.5		
15-4, 125	11.91	162.75	5.85	26		0.397	28	2.65	0.15	39	58	1.49	2.44	5.3		
16-1, 31	12.16	166.31	10.3	26	30	0.361	25	2.12	0.17	31	52	1.68	2.28	10.0		
16-1, 84	11.65	166.84	10.9	20	37	0.406	30	2.14	0.19	42	60	1.43	2.39	10.1		
16-1, 100	11.91	167.00	12.3	12	80	0.406	50	2.45	0.19	56	88	1.57	2.00	13.6		
16-1, 117	12.16	167.17	11.5	2	110	0.786	105	3.28	0.24	115	180	1.57	1.93	13.2	260 + 527	526 + 227
16-2, 87	11.91	168.37	5.11	29	47	0.324	33	2.70	0.12	42	68	1.62	2.19	5.2		
16-3, 78	11.91	169.78	4.07	50	35	0.224	28	2.24	0.10	28	53	1.89	2.69	3.4	166	117
16-4, 42	11.91	170.92	6.33	41	41	0.296	30	2.69	0.11	34	57	1.68	2.56	5.5		
16-4, 125	11.91	171.75	7.10	24	35	0.327	30	2.52	0.13	39	62	1.59	2.38	6.2		
17-1, 70	12.16	175.70	4.79	30	50	0.313	33	2.61	0.12	39	69	1.77	2.30	4.6		
17-2, 55	11.65	177.05	6.29	27	70	0.333	33	2.38	0.14	37	68	1.84	2.53	5.5	195	147
18-1, 16	11.65	184.16	7.69	36	38	0.338	33	2.41	0.14	39	65	1.67	2.13	8.0		
18-2, 84	11.91	186.34	15.0	51	63	0.569	43	2.59	0.22				2.00	16.7		
19-1, 78	12.16	193.78	20.2	54	68	0.649	38	3.25	0.20	51	69	1.35	2.32	19.4		
19-1, 108	11.65	194.08	11.3	−53	59	0.481	35	3.01	0.16	55	70	1.27	2.95	8.5		
19-1, 134	10.64	194.34	11.2	−45	68	0.461	35	3.55	0.13	45	81	1.80	2.97	8.4		
20-1, 39	11.91	197.89	8.75	53	40	0.381	25	2.93	0.13	39	56	1.44	2.58	7.6		
20-1, 143	11.91	198.93	10.7	53	35	0.374	25	2.67	0.14	34	55	1.62	2.50	9.5		
20-3, 17	11.65	200.17	14.1	50	47	0.530	35	2.79	0.19	45	62	1.38	2.28	13.8		
20-3, 141	11.65	201.91	19.6	53	37	0.569	27	2.99	0.19	45	55	1.22	2.45	17.7		
21-1, 95	11.15	202.95	12.5	44	44	0.367	33	2.29	0.16				2.42	11.4		
21-2, 33	11.91	203.83	6.72	58	40	0.314	28	2.62	0.12	34	58	1.71	2.69	5.6		
21-2, 78	12.06	204.28	8.24	53	35	0.335	26	2.58	0.13	39	53	1.36	2,54	7.2		
21-2, 111	11.91	204.61	6.79	55	39	0.299	25	2.30	0.13	34	54	1.59	2.67	5.6		
21-3, 69	11.91	205.69	15.8	54	41	0.444	30	2.96	0.15	53	58	1.09	2.18	16.1		
22-1, 83	11.65	211.83	19.0	49	32	0.425	23	2.36	0.18	34	46	1.35	2.28	18.6		
22-2, 32	11.91	212.82	13.5	53	40	0.393	27	2.31	0,17	37	45	1.22	2.38	12.6	195	125
22-3, 99	12.16	214.99	14.9	41	47	0.453	35	2.16	0.21	45	65	1.44	1.89	17.6		
22-4, 57	11.40	216.07	6.46	53	47	0.350	30	2.50	0.14	31	60	1.94	2.40	6.0		
24-1, 43	11.91	224.93	6.33	43	57	0.325	30	2.95	0.11	39	63	1.62	3.01	4.7		
24-2, 106	11.40	227.06	6.57	47	45	0.345	28	3.14	0.11	34	61	1.79	3.45	4.2		
24-3, 70	11.40	228.20	6.40	47	57	0.345	25	3.14	0.11	31	55	1.77	3.43	4.2	227	133
Hole 482C																
9-1, 113	11.91	133.13	3.61	30	55	0.441	50	4.41	0.10	42	78	1.86	4.74	1.7		
9-1, 138	11.50	133.38	5.59	31	81	0.321	30	3.21	0.10	34	62	1.82	3.28	2.4		
10-2, 58	11.65	141.08	4.27	27	57	0.330	30	4.13	0.08	23	52	2.26	3.57	2.7	424	147
10-2, 61	11.91	141.11	4.02	28	53	0.314	28	3.14	0.10	32	55	1.72	3.62	2.5		
10-2, 78	11.91	141.28	4.10	30	64	0.331	35	3.31	0.10	34	58	1.71	3.87	2.4		
10-3, 119	11.65	143.13	4.07	−30	70	0.362	30	3.62	0.10	34	65	1.91	3.34	2.6		
11-1, 97	11.40	148.97	2.08	28	41	0.218	30	2.18	0.10	39	73	1.87	2.16	2.1	371	361
11-2, 11	11.65	149.61	5.30	37	66	0.315	30	2.63	0.12	37	62	1.68	2.70	4.4		
11-2, 44	11.40	149.94	0.55	36	55	0.096	30	1.07	0.09	34	67	1.97	1.34	0.9		
11-3, 26	11.65	151.26	4.74	35	62	0.227	33	2.52	0.09	31	64	2.06	3.25	3.2		
11-3, 63	11.65	151.63	4.05	36	54	0.195	30	2.17	0.09	25	58	2.32	3.33	2.7		
11-3, 128	11.76	152.28	4.53	38	54	0.189	30	2.36	0.08	28	62	2.21	3.09	3.3		
11-4, 107	11.40	153.57	5.26	37	59	0.263	35	2.63	0.10	37	63	1.70	2.75	4.3		
12-1, 39	11.76	157.39	3.58	12	45	0.340	30	2.43	0.14	39	55	1.41	2.70	2.9		
12-1, 146	11.76	158.46	3.39	14	34	0.329	25	2.35	0.14	37	58	1.57	2.61	2.9	197	152
12-2, 92	11.30	159.42	3.30	11	45	0.356	35	2.74	0.13	39	63	1.62	2.40	3.1		
13-1, 56	11.65	162.06	5.96	11	50	0.382	35	2.39	0.16	39	64	1.64	2.33	5.7		
13-2, 17	11.65	163.17	3.28	11	72	0.421	43	3.01	0.14	56	96	1.71	2.17	3.4		
13-2, 96	12.16	163.96	2.62	9	81	0.350	43	2.69	0.13	45	79	1.76	2.28	2.6		
13-3, 25	11.40	164.75	3.07	27	37	0.297	38	2.97	0.10	34	65	1.91	2.43	2.8		
13-3, 80	11.50	165.30	2.60	26	30	0.313	27	3.13	0.10	34	63	1.85	2.91	2.0		
13-3, 132	11.15	165.82	2.80	19	53	0.270	30	2.70	0.10	34	60	1.76	2.85	2.2		
14-1, 44	11.50	166.44	4.90	7	73	0.259	50	2.16	0.12	34	83	2.44	2.76	3.9	164	109
14-2, 22	11.81	167.27	4.25	13	46	0.274	30	2.11	0.13	36	57	1.58	2.38	4.0		
14-2, 131	11.76	168.81	5.02	11	43	0.282	32	2.35	0.12	28	56	2.00	2.52	4.4		
14-3, 77	11.65	169.77	3.68	17	33	0.275	23	2.29	0.12	28	61	2.18	2.71	3.1		
14-3, 122	11.40	170.22	2.63	27	35	0.238	25	1.98	0.12	28	46	1.64	2.53	2.3		
14-4, 61	11.65	171.11	2.49	32	43	0.243	28	2.43	0.10	25	47	1.88	2.58	2.1		
14-4, 132	11.40	171.82	2.46	27	29	0.248	30	2.25	0.11	28	56	2.00	2.92	1.9		
14-5, 46	11.40	172.46	2.10	36	50	0.293	32	2.44	0.12	37	69	1.86	2.42	1.9		
15-1, 42	11.91	175.42	2.76	18	50	0.310	33	3.10	0.10	34	68	2.00	2.37	2.6	229	182
15-2, 11	11.76	176.61	8.35	18	40	0.480	30	2.53	0.19	45	58	1.29	1.98	9.4		
15-2, 92	11.65	177.42	5.43	15	45	0.368	25	2.30	0.16	34	55	1.62	2.23	5.4		
15-4, 68	11.91	180.18	3.42	14–18	50	0.299	30	2.30	0.13	35	48	1.37	2.44	3.0		
15-4, 117	11.15	180.67	3.68	21	37	0.321		2.29	0.14	37	53	1.43	2.52	3.3		
Hole 482 D																
8-1, 10	11.15	139.06	4.39	24	385	1.71	330	3.98	0.43	326	443	1.36	1.80	5.57	519	529
9-1, 51	11.40	142.01	3.96	25	490	1.90	420	4.04	0.47	405	558	1.38	1.75	5.03		
9-2, 106	11.15	144.06	6.74	26	229	1.02	145	4.43	0.23	118	174	1.74	3.15	4.75		
9-3, 23	11.65	144.73	6.16	25	108	0.583	60	3.43	0.17				3.27	4.19		
9-3, 54	11.65	145.04	5.88	26	109	0.569	60	3.35	0.17	59	82	1.39	2.95	4.42		
10-1, 69	10.89	151.19	17.0	40	78	0.508	36	3.63	0.14	45	81	1.80	3.41	11.1		
10-2, 11	11.15	152.11	8.81	31	85	0.397	41	3.31	0.12	34	58	1.71	3.24	6.0		
10-2, 57	10.89	152.57	4.76	32	50	0.239	20	2.66	0.09	23	28	1.22	3.35	3.16	326	98
10-2, 111	11.65	153.11	3.53	40–42	61	0.278	23	3.09	0.09	28	43	1.54	3.11	2.5		
10-3, 18	11.40	153.68	3.48	37	58	0.267	25	2.97	0.09	30	45	1.50	3.23	2.39		
10-3, 109	11.40	154.59	15.92	16	145	0.655	47	1.82	0.36	107	134	1.25	1.08	32.9		
11-1, 128	10.64	160.78	15.88	22	107	0.632	65	1.98	0.32	82	82	1.00	1.17	30.2		
11-3, 80	11.40	163.30	10.25	24	68	0.542	40	1.94	0.28	62	78	1.26	1.38	16.54	190	133
12-1, 27	11.65	168.77	4.50	13	59	0.338	36	2.11	0.16	39	69	1.77	1.95	5.1		
12-1, 65	11.65	169.15	5.82	19	53	0.361	30	2.12	0.17	39	58	1.49	1.97	6.6		

Table 1. (Continued).

Sample (level in cm)	Vol. (cm^3)	Depth (m)	J_{NRM} ($\times 10^{-3}$ gauss)	I (°)	MDF(1) (Oe)	J_{RS} (gauss)	MDF(2) (Oe)	J_S (gauss)	J_{RS}/J_S	H_C (Oe)	H_{RC} (Oe)	H_{RC}/H_C	χ ($\times 10^{-3}$ gauss)	Q	T_c (heating) (°C)	T_c (cooling) (°C)
Hole 482D (Cont.)																
12-1, 119	11.65	169.69	6.00	30	50	0.356	32	1.78	0.20	45	66	1.47	1.71	7.81	155	111
12-2, 86	11.65	170.86	20.4	2	80	0.683	50	2.97	0.23	65	88	1.35	2.18	20.81		
12-3, 21	11.65	171.71	10.2	4	57	0.505	30	2.40	0.21	45	63	1.40	1.88	12.0		
12-3, 61	11.65	172.11	11.5	5	55	0.438	30	2.43	0.18	37	61	1.65	2.28	11.2		
12-3, 122	11.27	172.72	3.25	9	75	0.342	28	2.28	0.15	34	61	1.79	2.65	2.7		
12-4, 45	11.00	173.45	17.99	6	62	0.706	38	2.82	0.25	53	77	1.45	62.0	19.4		
13-1, 127	10.89	178.77	6.99	14	45	0.543		2.72	0.20	42	62	1.48	45.0	7.5		
13-2, 12	11.15	179.12	9.66	18	77	0.846	55	2.58	0.25	64	87	1.36	1.82	11.8	258	168
13-3, 33	9.63	186.83	2.41	25	52	0.299		2.49	0.12	32	57	1.78	2.62	2.0		
Hole 482F																
4-3, 129	11.65	136.79	9.30	41	65	0.353	32	2.52	0.14	38	68	1.79	2.85	7.3		
5-1, 7	11.40	142.07	9.79	43	42	0.329	25	2.53	0.13	35	55	1.57	3.04	7.2		
5-1, 141	11.40	143.41	11.35	34	47	0.395	30	2.47	0.16	41	52	1.27	2.85	8.9		
Hole 483										39	69	1.77	2.40	6.1		
										32	67	2.09	2.76	4.8		
13-4, 13	11.30	110.13	6.63	32	68	0.303	35	2.53	0.12	39	63	1.62	2.31	5.1		
13-4, 89	10.64	110.89	5.91	36	65	0.735	37	2.14	0.11	45	68	1.51	2.12	4.5		
14-1, 31	11.65	115.31	5.33	−23	55	0.274	30	1.61	0.17	48	70	1.46	1.91	6.1		
14-1, 83	9.98	115.83	4.28	±29	94	0.298	35	1.99	0.15	34	70	2.06	2.13	2.6		
14-2, 10	11.45	116.60	5.25	−26	75	0.308	40	1.93	0.16	31	70	2.26	2.43	3.6		
14-2, 53	10.39	117.03	2.47	−18	75	0.230	35	1.77	0.13	25	45	1.80	2.46	2.7		
14-2, 106	11.25	117.56	3.92	±21	110	0.232	37	1.78	0.13	28	57	2.04	2.03	2.4		
15-1, 20	11.40	124.20	3.03	?	18	0.170	23	1.70	0.10	25	58	2.32	2.36	2.8		
15-1, 102	10.39	125.02	2.23	−16	57	0.193	25	1.48	0.13	39	72	1.85	2.51	3.0		
15-2, 99	11.40	126.49	3.01	−11	45	0.206	25	1.87	0.11	35	63	1.80	2.42	3.3		
15-3, 4	11.50	127.04	3.42	−36	80	0.279	35	2.33	0.12	30	62	2.07	2.36	0.9		
16-1, 54	11.25	133.54	3.62	−38	67	0.254	35	2.12	0.12	30	62	2.07	2.37	2.2		
16-1, 112	11.25	134.12	1.21	−34	107	0.238	30	2.16	0.11	28	60	2.14	2.62	2.1	182	141
16-1, 138	11.65	134.38	2.38	−34	70	0.228	33	1.90	0.12	37	80	2.16	2.35	3.8		
16-2, 14	11.35	134.64	2.53	−26	59	0.208	34	2.08	0.10	38	78	2.05	2.34	1.8		
16-2, 62	11.40	135.12	3.98	−34	81	0.280	37	2.15	0.13	68	103	1.51	1.24	2.8		
16-2, 140	11.65	135.90	1.85	−36	100	0.262	35	2.18	0.12	35	108	3.09	1.29	2.5		
17-1, 60	11.55	142.60	1.59	−40	91	0.155	60	1.29	0.12	53	113	2.13	1.18	5.1		
17-2, 30	10.24	143.80	1.46	−40	90	0.143	50	1.19	0.12	45	93	2.07	1.14	3.6		
17-2, 96	10.13	144.46	2.71	−40	96	0.190	62	1.36	0.14	44	94	2.14	1.23	3.7		
17-3, 20	9.98	145.20	1.85	−44	130	0.179	56	1.28	0.14	32	63	1.97	2.21	2.7		
18-4, 110	11.65	156.60	2.03	49	75	0.191	43	1.36	0.14	44	68	1.55	2.30	18.3		
18-4, 148	11.15	157.08	2.72	−22	85	0.270	30	2.08	0.13	84	110	1.31	1.22	35.4	158	139
20-1, 14	10.29	169.14	18.9	−48	102	0.473	35	2.25	0.21							
20-1, 110	12.16	170.10	19.4	−42	138	0.758	60	1.99	0.38							
20-1, 142	11.40	170.42	18.8	−44	100	0.631	45	2.04	0.31	59	83	1.41	1.73	24.0		
20-2, 22	10.13	170.72	12.4	−48	122	0.500	35	2.00	0.25	42	64	1.52	2.12	13.0		
20-3, 29	10.64	178.29	21.1	−43	82	0.673	43	2.10	0.32	68	82	1.21	1.61	29.1		
21-1, 106	11.40	179.06	7.32	−47	138	0.492	33	2.24	0.22	45	63	1.40	2.31	7.0		
21-2, 4	11.15	179.54	17.3	−50	80	0.552	30	2.04	0.27	45	73	1.62	1.99	19.3		
21-2, 39	11.00	179.89	18.7	−47	130	0.732	50	2.03	0.36	79	81	1.03	1.24	33.6		
21-2, 124	10.89	180.84	12.3	−50	90	0.539	33	2.07	0.26	48	65	1.35	1.89	14.5		
22-1, 84	11.40	183.34	24.4	−39	155	0.735	82	1.67	0.44				0.92	59.2		
22-1, 135	9.98	183.85	28.5	−50	185	0.635	117	1.35	0.47	132	172	1.30	0.648	97.8	220	189
22-2, 77	7.88	184.77	25.8	−49	339	0.527	230	0.92	0.57	248	318	1.28	0.35	163.0		
22-3, 103	10.13	186.53	22.5	−49	265	0.562	180	0.94	0.60	183	270	1.48	0 43	117.0	227	192
22-4, 35	11.40	187.35	24.5	−34	122	0.622	65	1.68	0.37				1.92	53.2		
22-4, 103	11.25	188.02	8.43	−35	93	0.443	43	2.46	0.18	52	86	1.65	2.13	8.8		
23-1, 64	11.65	187.64	25.5	−36	78	0.548	47	1.89	0.29	62	76	1.23	1.50	37.9	162	128
23-1, 113	9.88	188.13	14.1	−42	90	0.390	33	1.77	0.22	41	65	1.59	2.02	15.5		
23-2, 37	11.65	188.87	10.3	−43	110	0.426	30	1.94	0.22	48	70	1.46	1.82	12.5		
23-2, 120	9.83	189.70	19.9	−29	230	0.717	135	1.49	0.48	169	215?	1.27	0.70	63.5		
24-1, 48	11.25	191.98	7.52	−31	76	0.523	40	3.08	0.17	51	84	1.65	2.28	7.3		
24-2, 4	11.30	193.04	13.9	−32	85	0.424		2.65	0.16	39	68	1.74	2.87	10.7		
24-2, 61	11.55	193.61	6.95	−28	80	0.388	30	2.59	0.15	31	57	1.84	3.52	4.4	132	107
25-1, 24	11.20	196.24	31.2	−28	92	0.649	50	2.60	0.25	93	105	1.13	1.97	35.3	205	169
25-1, 84	12.16	196.84	14.9	−33	83	0.443	33	2.46	0.18	37	62	1.68	3.09	10.7		
25-2, 74	11.65	198.24	5.89	−31	67	0.327	34	2.73	0.12	31	65	2.10	3.15	4.1		
26-1, 11	12.06	200.11	7.88	−32	74	0.382	38	2.94	0.13	41	60	1.46	2.99	5.9		
26-1, 138	12.26	201.38	5.22	−30	81	0.456	35	3.26	0.14	46	69	1.50	2.37	4.9		
26-2, 13	10.44	201.63	6.55	−34	122	0.445	43	2.62	0.17	52	88	1.69	2.55	5.7		
26-2, 60	10.39	202.10	28.5	−35	82	0.681	46	2.62	0.26	62	87	1.40	1.70	36.1		
26-3, 8	12.16	203.80	16.2	−33	128	0.443	50	2.61	0.17	46	89	1.93	2.63	13.8	164	132
26-3, 118	10.64	204.18	6.34	−34	106	0.387	20	2.76	0.14	28	60	2.14	3.30	4.3		
Hole 483B																
2-7, 91	10.74	110.91	8.14	27	75	0.242	40	2.20	0.11	35	85	2.43	2.76	6.5		
3-1, 46	10.69	110.96	7.28	29	77	0.241	37	2.41	0.10	35	88	2.51	2.82	5.7		
3-1, 121	10.13	111.71	6.05	−22	115	0.268	54	2.23	0.12	42	88?	2.10	2.23	6.0	166	133
4-1, 64	9.93	120.14	2.27	−16	82	0.202	40	2.24	0.09	32	68	2.13	2.31	2.2		
4-2, 83	11.15	121.83	2.13	−12	54	0.170	30	1.70	0.10	23	63	2.74	2.40	2.0		
4-3, 127	10.94	123.77	2.38	−16	64	0.175	30	1.75	0.10	28	63	2.25	2.20	2.4		
4-4, 111	11.15	125.11	1.31	−12	115?	0.137	30	1.52	0.09	24	60	2.50	2.22	1.1	141	107
4-5, 94	11.05	126.44	2.03	−19	100?	0.172	35	1.72	0.10	31	74	2.42	2.14	2.1		
4-7, 4	11.25	128.54	2.64	−18	71	0.210	32	1.50	0.14	31	69	2.23	2.30	2.5		
Hole 485A																
11-3, 79	11.15	149.29	2.90	32	62	0.302	34	1.51	0.20	39	80	2.05	1.51	4.28		
12-1, 59	11.18	155.59	12.47	49	65	0.762	47	3.18	0.24	60	80	1.33	2.62	10.57	166	122
13-1, 96	11.40	158.96	6.42	49	40	0.437	30	2.73	0.16	35	65	1.86	3.35	4.26		
14-1, 60	11.65	160.10	7.48	42	60	0.432	45	2.54	0.17	35	70	2.0	3.17	5.25		
17-1, 108	11.15	182.30	10.06	31	90	0.503	57	3.59	0.14	51	115	2.25	2.80	7.97	222	182
17-2, 77	10.89	183.77	9.16	33	64	0.281	32	2.55	0.11	28	65	2.32	4.29	4.74		
18-2, 29	11.15	183.79	7.21	31	43	0.286	23	2.60	0.11	24	55	2.29	4.46	3.59		
23-1, 99	11.15	212.49	8.07	36	70	0.373	38	3.39	0.11	46	94	2.04	3.60	4.98		
23-4, 12	10.89	216.12	6.60	32	43	0.433	28	3.61	0.12	39	60	1.54	2.49	4.2		
24-2, 21	11.40	217.71	5.08	55	62	0.248	35	2.76	0.09	31	85	2.74	2.97	3.80		
25-2, 29	10.89	222.79	6.92	46	55	0.278	31	2.78	0.10	31	67	2.16	4.0	3.84		
25-3, 29	10.89	225.29	7.15	44	70	0.347	37	3.15	0.11	37	85	2.30	3.42	4.64		
29-1, 20	11.40	239.70	1.87	38	155	0.174	155	0.92	0.19	104	274	2.63				
29-2, 123	11.15	242.23	3.78	20	179	0.388	85	3.88	0.10	70?	160	2.29	2.66	3.16	501	379

Table 1. (Continued).

Sample (level in cm)	Vol. (cm^3)	Depth (m)	J_{NRM} ($\times 10^{-3}$ gauss)	I (°)	MDF(1) (Oe)	J_{RS} (gauss)	MDF(2) (Oe)	J_S (gauss)	J_{RS}/J_S	H_C (Oe)	H_{RC} (Oe)	H_{RC}/H_C	χ ($\times 10^{-3}$ gauss)	Q	T_c (heating) (°C)	T_c (cooling) (°C)
Hole 485A (Cont.)																
29-4, 48	11.15	244.48	7.03	30	117	0.385	40	3.50	0.11	45	105	2.33	3.68	4.25		
30-1, 43	11.15	249.93	9.34	24	155	0.474	70	2.49	0.19	62	127	2.05	3.26	6.36	269+512	217
30-3, 105	11.40	253.55	5.60	19	75	0.281	36	3.12	0.09	38	83	2.18	2.98	4.17		
31-2, 85	11.15	256.85	5.77	20	115	0.415	62	3.46	0.12	60	110	1.83	2.89	4.44		
32-1, 10	10.89	259.10	5.30	25	140	0.286	75	2.60	0.11	53	138	2.60	2.41	4.90	293+482	262
32-3, 58	10.89	262.55	2.25	22	123?	0.247	50	2.06	0.12	27	107	3.96	3.09	1.62		
32-5, 138	11.40	266.38	3.18	22	130	0.264	56	3.30	0.08	45	118	2.62	3.07	2.30		
32-6, 69	11.15	267.19	2.37	22	148	0.239	50	2.99	0.08	38	110	2.89	3.01	1.75		
33-2, 81	11.15	270.31	2.64	25	110	0.306	75	3.40	0.09	62	170	2.74	2.55	1.99		
34-2, 68	11.15	274.18	6.79	39?	34	0.268	22	2.98	0.09	27	47	1.74	3.49	4.33	182	122
35-1, 26	11.15	286.26	6.40	38	45	0.260	25	2.60	0.10	24	53	2.21	3.98			
35-3, 72	11.40	289.72	6.29	38	55	0.281	25	2.81	0.10	28	59	2.10	3.77	3.7		
35-4, 47	11.15	290.97	5.38	39	45	0.256	23	2.33	0.11	27	57	2.11	3.38	3.53		
35-6, 44	11.15	293.94	5.68	38	40	0.283	23	2.18	0.13	25	53	2.12	3.21			
38-2, 67	11.40	315.17	0.83	−55	135	0.472	65	2.78	0.17	79	115	1.46	2.20	0.84		
38-4, 102	11.15	318.52	1.16	−43	22	0.284	42	2.58	0.11	37	88	2.38	2.86	0.90		
38-6, 35	11.65	320.85	2.31	64	35	0.307	30	3.07	0.10	32	64	2.0	3.22	1.60	253	158
39-2, 77	11.15	324.27	2.78	?	28	0.410	23	3.15	0.13	32	57	1.78	3.13	1.97		
39-4, 27	11.40	326.72	2.98	?	40	0.393	27	3.02	0.13	30	60	2.0				
39-5, 8	11.40	328.80	1.14	?	20	0.340	33	2.83	0.12	39	66	1.69	2.71	0.93	273	197

Note: J_{NRM} = natural remanent magnetization; I_0 = stable inclination; MDF(1) = mean destruction field from isothermal remanence demagnetization; J_S = saturation magnetization; H_C = coercive force; H_{RC} = remanent coercive force; χ = susceptibility; Q = Koenigsberger ratio based on a magnetic field H_0 = 0.45 Oe; T_c (heating) = Curie temperature from heating curve; T_c (cooling) = Curie temperature from cooling curve.

400°C during heating, followed by an increase in magnetization between 400°C and 500°C, which falls off to zero at about 550°C. After cooling, furthermore, the magnetization usually increases by a factor of two or more. These features were not observed in any of our samples.

We performed a number of tests to exclude the possibility that this effect was due to our measuring technique. For the heating rate (40°C/min.), only a small contribution (<20°C) could be attributed to instrument error, and the data in Table 1 and in the figures have been corrected accordingly. It should also be noted that similar thermomagnetic properties have been reported for Leg 65 basalts by Pechersky et al. (this volume).

Microscope Observations

We made polished sections from the same samples that were used for thermomagnetic analysis. In all samples, the predominant opaque mineral is titanomagnetite, the volume content of which varies from about 0.5% in the pillow basalts to about 5% in the flow units. The grain size of the opaques in the pillow basalts ranges from below the limit of optical resolution to about 10 μm, and the grains are typically anhedral. Coarser-grained opaques occur in the flow units where grain size averages several tens of microns and occasionally reaches several hundred microns. Skeletal-to-subhedral forms are most abundant, and inclusions could be seen in many of the larger grains. Some samples from the flow units had a second, finer-grained titanomagnetite fraction (10 μm or less) in the matrix. Most of the titanomagnetite grains appeared to be homogeneous and features associated with low temperature oxidation, such as curved and branching cracks, are clearly developed only in a few samples showing a high Curie temperature.

In some samples, ilmenite occurs as separate primary laths. Ilmenite is also present as a secondary mineral in Sections 482D-8-1, 106 cm and 482B-16-1, 117 cm. It is not a result of high temperature deuteric oxidation in this instance, since there are no systematic lamellae present. Instead, there is an irregular intergrowth within the host titanomagnetite, indicating that it was produced by decomposition of titanomaghemite (perhaps because of hydrothermal activity).

Saturation Magnetization (J_S) and Saturation Isothermal Remanence (J_{RS})

The variation in saturation magnetization both within and between holes is very small. This can be seen in the average values given in Table 2 as well as in the individual measurements listed in Table 1. The saturation magnetization averages 2.0 gauss, a value close to the mean value found for unoxidized samples from Leg 49 (Day et al., 1979). There is a greater variation in the saturation isothermal remanence values; but this is to be expected since J_{RS} is dependent on grain size and shape as well as on composition and concentration, whereas J_S is independent of grain size, although it is related to grain size by oxidation, when oxidation has taken place. The distribution of J_{RS}/J_S values is shown in Figure 2. The majority of the samples have values of 0.1 to 0.2, indicating pseudo single domain grains. There is only one peak in the Leg 65 histogram whereas the Leg 49 histogram was bimodal. Again, it is apparent that only relatively fresh titanomagnetites are found in the Leg 65 basalts. Many of the high J_{RS}/J_S values are associated with pillow basalts, as would be expected since they contain much finer titanomagnetite grains.

Coercive Force (H_C), Remanent Coercive Force (H_{RC}), and Mean Destructive Field (MDF)

Figures 3 and 4 show the distributions of H_C and H_{RC}, and the distribution of the ratio H_{RC}/H_C is shown in Figure 5. These values are typical of large pseudo single domain titanomagnetites. According to a theory proposed by Stoner and Wohlfarth (1948), in the limiting case of a random assemblage of identical, noninteracting single domain grains, $H_{RC}/H_C = 1.09$. As grain size increases through the pseudo single domain range, H_{RC}/H_C increases to about 3. For values of H_{RC}/H_C greater than 3, one is looking at predominantly multidomain grains. In the absence of H_{RC} and H_C measure-

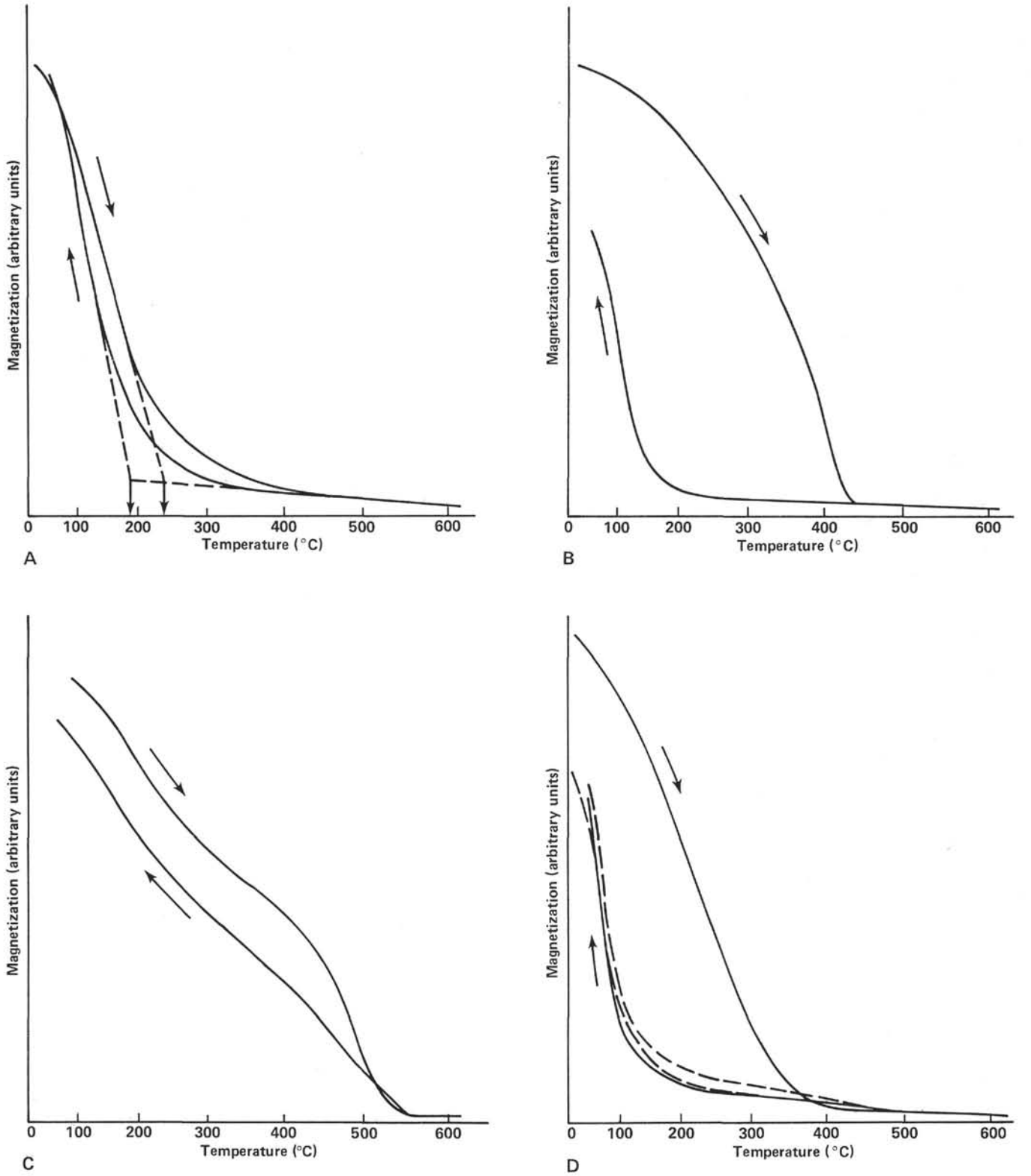

Figure 1. Variation of magnetization with temperature for representative samples. (Heating and cooling curves are indicated by arrows.) (A) Thermomagnetic curve showing reversible behavior (Section 485A-17-1, 108). Broken lines denote the graphical method of Curie temperature determination; (B) curve showing irreversible behavior (Section 482C-10-2, 58); (C) two Curie temperature curves (Section 482B-16-1, 117); (D) irreversible curve showing almost perfect reversibility of second heating and cooling cycle (Section 482D-10-2, 57).

Table 2. Average magnetic properties of basalts for each hole drilled on Leg 65.

Hole	MDF(1) (Oe)	J_{RS} (gauss)	MDF(2) (Oe)	J_S (gauss)	J_{RS}/J_S	H_C (Oe)	H_{RC} (Oe)	H_{RC}/H_C	χ (gauss/Oe)	Q
482B	53	0.409	38	2.54	0.17	47	70	1.55	2.38	12.2
482C	51	0.301	31	2.64	0.12	35	62	1.82	2.75	3.2
482D	110	0.605	68	2.81	0.21	79	111	1.48	6.62	9.8
482F	51	0.359	29	2.51	0.14	38	58	1.54	2.91	7.8
483	102	0.414	49	2.04	0.21	51	87	1.83	2.03	19.3
483B	84	0.202	36	1.92	0.11	31	73	2.38	2.37	3.4
485A	79	0.344	45	2.84	0.12	42	92	2.19	3.14	3.8

Note: MDF(1) is the mean destructive field from NRM demagnetization; J_{RS} = saturation remanence; MDF(2) is mean destructive field from isothermal remanence demagnetization; J_S = saturation magnetization; H_C = coercive force; H_{RC} = remanent coercive force; χ = susceptibility; Q = Koenigsberger ratio based on a magnetic field $H_0 = 0.45$ Oe.

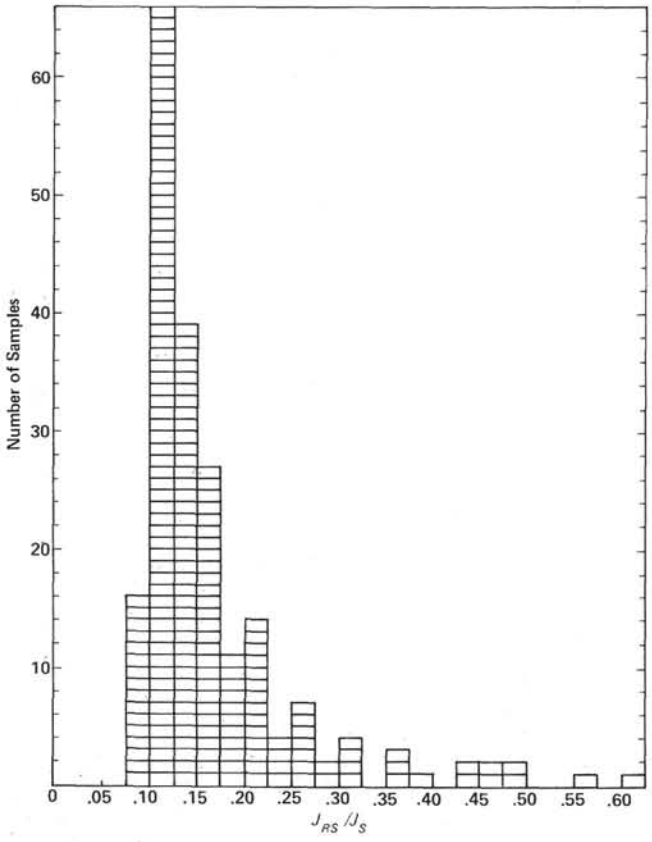

Figure 2. Histogram of the ratio J_{RS}/J_S (all sites).

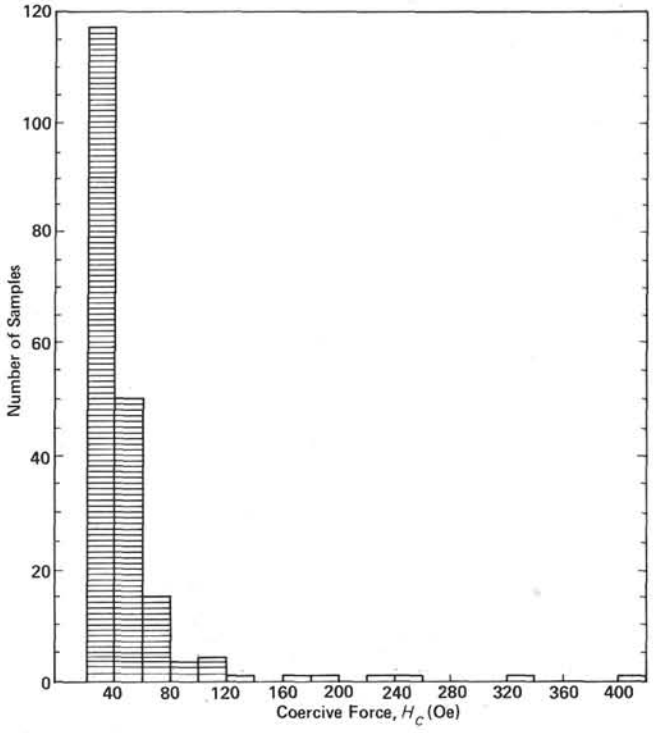

Figure 3. Histogram of coercive force, H_C (all sites).

ments, the median destructive field (MDF) has commonly been used to estimate the coercivity distribution. Two MDFs are listed in the tables. MDF(1) is the median destructive field from the NRM demagnetization curve, and MDF(2) is from the saturation isothermal remanence demagnetization curve. The observation that MDF(1) is generally greater than MDF(2) again indicates the presence of pseudo single domain grains on the basis of the Lowrie-Fuller test.

Other Magnetic Measurements

The paleomagnetic results for the Leg 65 basalts have been presented elsewhere (Day, this volume). For completeness we have shown the distributions of NRM, the Koenigsberger ratio (Q), and stable inclination (I_0) in Figures 6, 7, and 8.

Several samples were selected for thermal demagnetization studies (Day, this volume). Although the temperature dependence of the NRM appears to be valid, the stable inclinations determined from the demagnetization curves are noticeably different from those found in neighboring samples that were AF demagnetized.

DISCUSSION

The Curie temperature of a completely unaltered oceanic basalt should be about 125°C (Peterson et al., 1979). Since the variability of the primary composition (i.e., the presence of minor constituents such as Mg, Al, and Cr) is limited in submarine basalts, we can expect an unaltered oceanic basalt to have a Curie temperature of 125°C with a variation of about ±50°C from this value. The Curie temperatures obtained from the cooling curves in our thermomagnetic experiments fall within this range. Values obtained from the heating curves, however, are systematically higher. In fact, the difference, ΔT_c, between the two Curie temperatures (a

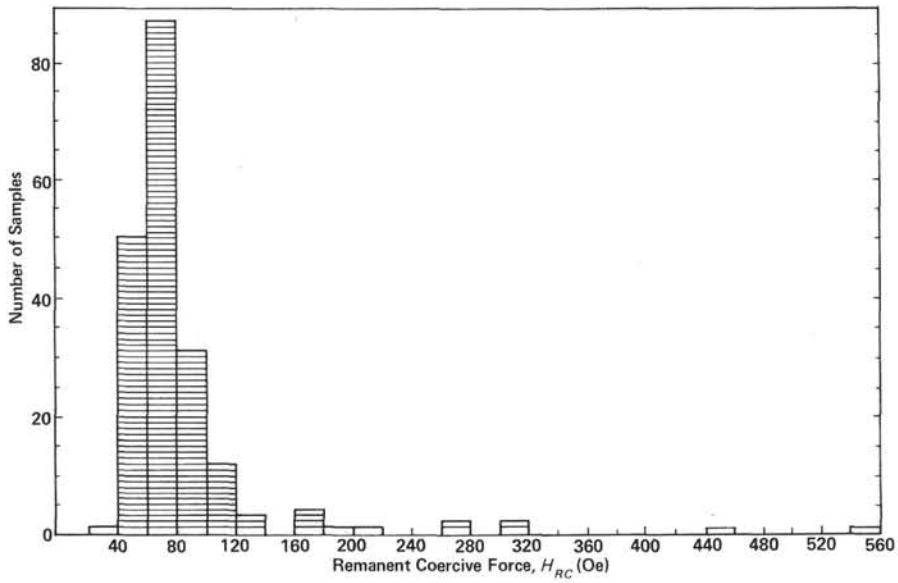

Figure 4. Histogram of remanent coercive force, H_{RC} (all sites).

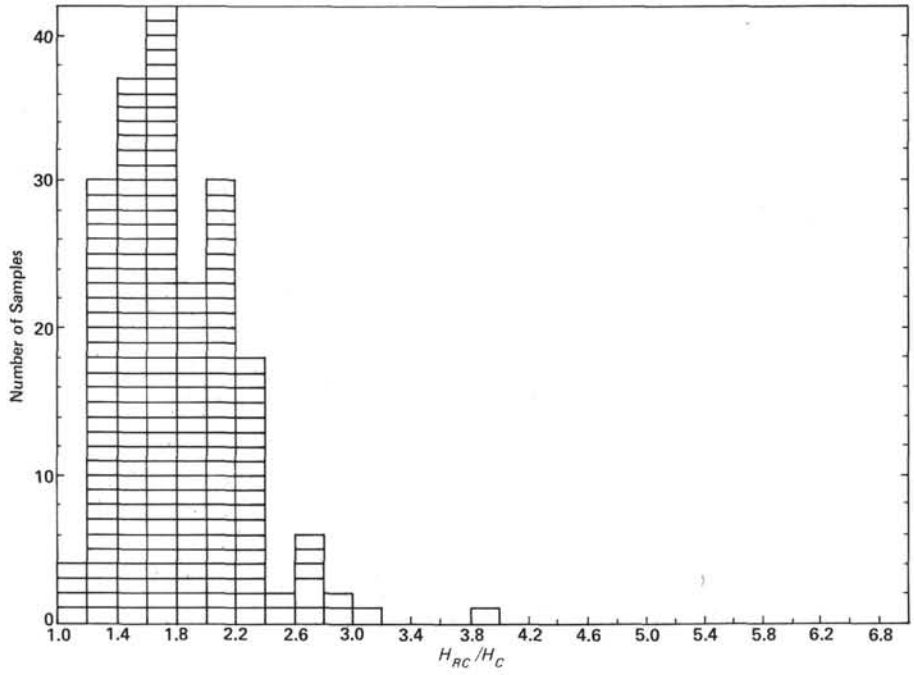

Figure 5. Histogram of the ratio H_{RC}/H_C (all sites).

measure of the degree of irreversibility), increases with increasing Curie temperature (Fig. 9). The most likely interpretation for this would be a variable degree of alteration, despite the young age of the Leg 65 basalts.

It is well known that submarine weathering leads to maghemitization (i.e., low-temperature oxidation) of titanomagnetite grains. The metastable alteration product, a cation-deficient spinel phase, has a higher Curie temperature than the original titanomagnetite. Using data obtained from synthetic samples, many authors have used the increase in Curie temperature to determine the degree of oxidation (assuming a uniform original composition). It has been shown, however, (Johnson and Melson, 1978; Peterson et al., 1979) that the low-temperature oxidation is essentially accomplished by Fe-migration out of the titanomagnetite. Hence the original Fe/Ti ratio will not be preserved. Our thermomagnetic results show that a chemical change takes place during the first heating, and that the metastable titanomaghemite is reduced to a stable stoichiometric(?) titanomagnetite because of the low oxygen fugacity. On repeated heatings (Fig. 1D), the behavior is always reversible, but subsequent Curie temperatures are lower than the initial Curie temperature. With the aid of

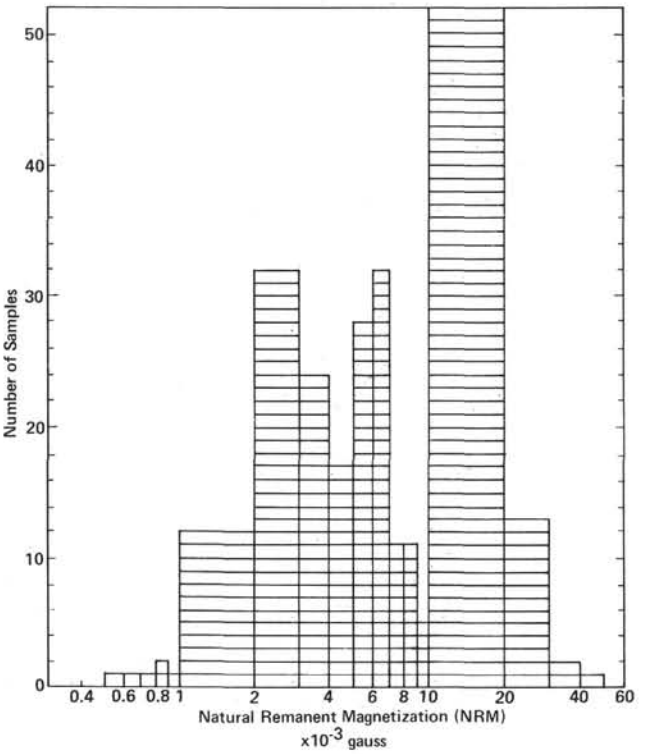

Figure 6. Histogram of NRM intensity (all sites).

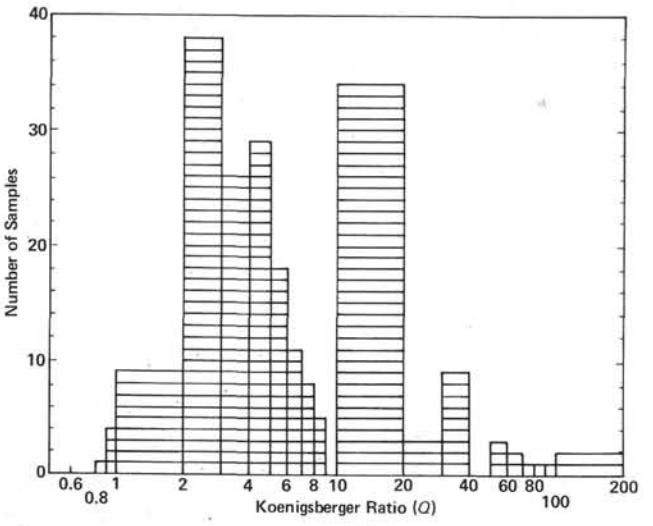

Figure 7. Histogram of Koenigsberger ratio, Q (all sites).

microprobe analyses, it should be possible to relate this difference to the amount of low temperature oxidation that took place. In the present instance, however, the anomalous behavior of the basalts may be due to the fact that the original titanomagnetite composition in the Leg 65 basalts is more variable than in other oceanic basalts. For example, samples from Cores 482C-11, 483-22, 485A-29, and 485A-39 appear to have unusually low initial titanium contents.

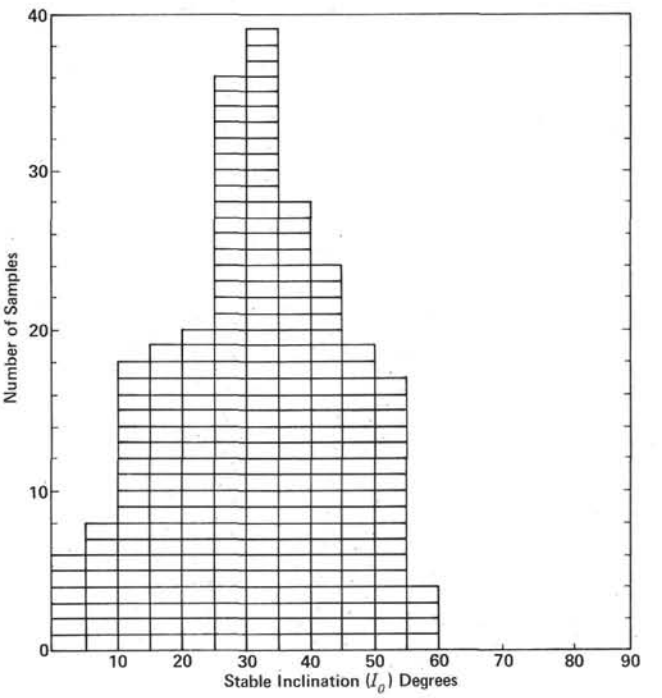

Figure 8. Histogram of stable inclination, I_0 (all sites).

Alteration is limited in the inner parts of the massive flow units, but for thinner cooling units, the maghemitization can be very high. Moreover, multiphase magnetic mineral assemblages occur in several samples (i.e., Cores 485A-29 through 32), and the titanomagnetites are completely decomposed in Sample 482D-8-1, 106 cm. In view of the young age of the basalts, such extremes may indicate the presence of hydrothermal activity and deuteric alteration.

The magnetic properties of the Leg 65 basalts are remarkably uniform. The only distinct differences reflect the finer grain size of the titanomagnetites in the pillow basalts. The titanomagnetites for the most part are fresh or slightly oxidized with an occasional example of extreme alteration. As can be seen in Figure 10, the magnetic grains fall in the pseudo single domain grain-size category, though grains in the pillow basalts approach single domain size. In comparing the magnetic properties of Leg 65 basalts with those from Leg 49 (Day et al., 1979), it becomes obvious that the Type II basalts found on Leg 49 are missing. While most of the Leg 49 magnetic properties exhibit bimodal distributions, the properties of basalts from Leg 65 each group around a single peak.

ACKNOWLEDGMENTS

We would like to thank the many people who were responsible for the success of DSDP Leg 65. We are particularly indebted to Barry Davis and Gretchen Green for help with some of the magnetic measurements. This research was partially funded by a grant from the National Science Foundation.

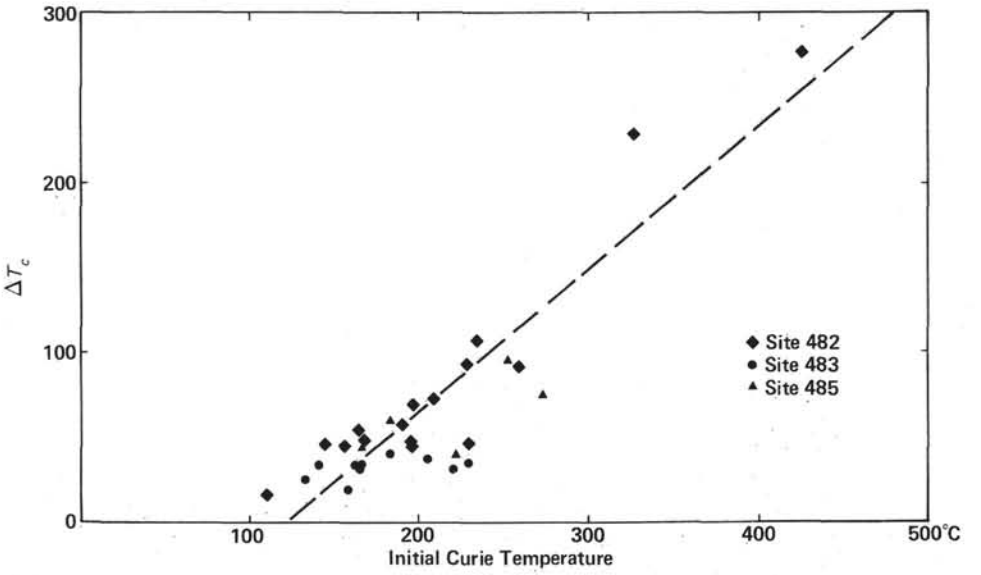

Figure 9. Difference, ΔT_c, of Curie temperatures based on heating and cooling curves versus initial Curie temperature based on heating curve. Broken line represents the visual best fit assuming a linear relationship.

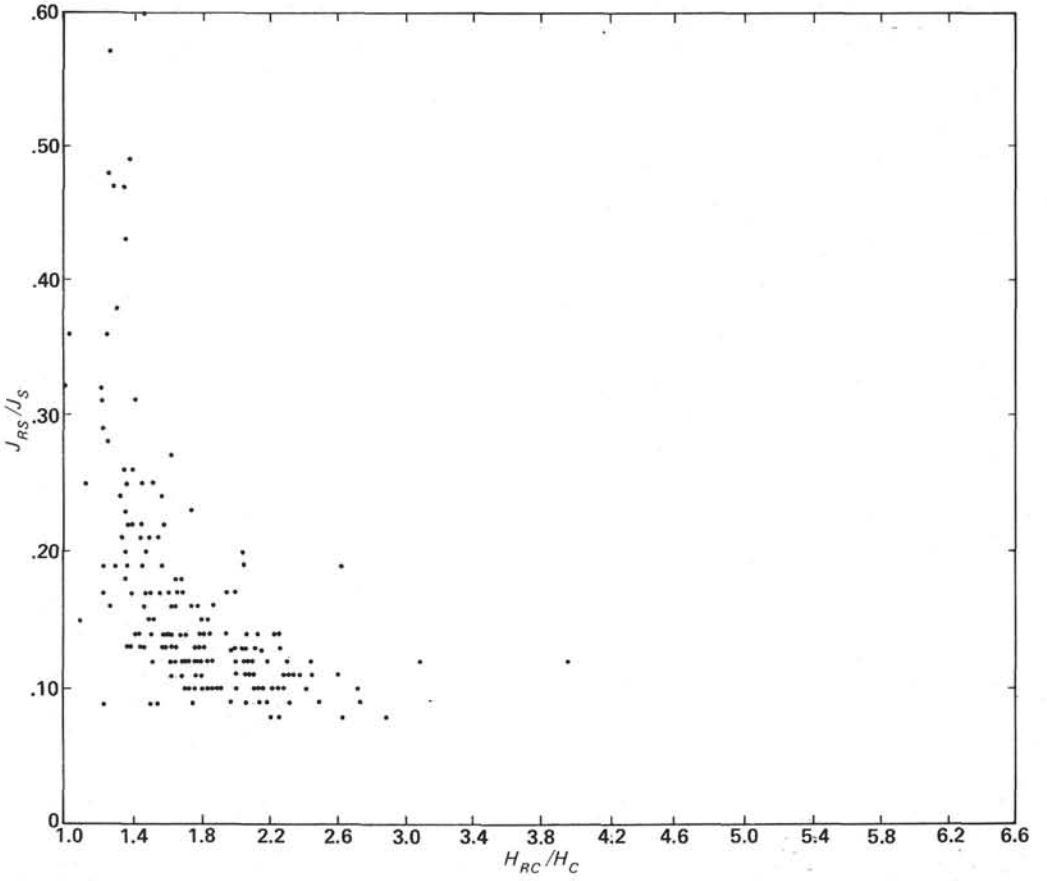

Figure 10. J_{RS}/J_S versus H_{RC}/H_C, (all sites).

REFERENCES

Day, R., Halgedahl, S., Steiner, M., et al., 1979. Magnetic properties of basalts from DSDP Leg 49. *In* Luyendyk, B. P., and Cann, J. R., et al., *Init. Repts. DSDP*, 49: Washington (U.S. Govt. Printing Office), 781–791.

Grommé, C. S., Wright, T. L., and Peck, D. L., 1969. Magnetic properties of iron-titanium oxide minerals in Alae and Makaopuhi lava lakes, Hawaii. *J. Geophys. Res.*, 74:5277–5293.

Johnson, H. P., and Melson, W. G., 1978. Electron microprobe analysis of some titanomagnetite grains from Hole 395A. *In* Melson, W. G., Rabinowitz, P. D., et al., *Init. Repts. DSDP*, 45: Washington (U.S. Govt. Printing Office), 575–580.

Kobayashi, K., and Fuller, M., 1967. Vibration magnetometer. *In* Collinson, D. W., Creer, K. M., and Runcorn, S. K. (Eds.), *Methods in Paleomagnetism:* New York (Elsevier), pp. 450–456.

Peterson, N., Eisenach, P., and Bleil, U., 1979. Low temperature alteration of the magnetic minerals in ocean floor basalts. *Am. Geophys. Union: Maurice Ewing Ser.*, 2:169.

Stoner, E. C., and Wohlfarth, E. P., 1948. A mechanism of magnetic hysteresis in heterogeneous alloys. *Philos. Trans. R. Soc. London, Ser. A*, 240:599–642.